

## Thermoluminescence associated with two-hole recombination centers

R. Chen<sup>a,\*</sup>, J.L. Lawless<sup>b</sup>, V. Pagonis<sup>c</sup>

<sup>a</sup> Raymond and Beverly Sackler School of Physics and Astronomy, Tel Aviv University, Tel Aviv 69978, Israel

<sup>b</sup> Redwood Scientific Incorporated, Pacifica CA94044-4300, USA

<sup>c</sup> Physics Department, McDaniel College, Westminster, MD21157, USA



### A B S T R A C T

A model of thermoluminescence (TL) is presented based on a double-occupancy hole-recombination center and a single-electron trap. The concepts of double-electron traps and double-hole centers have been established before with regard to different solid state phenomena and also mentioned as a possible occurrence in connection with TL. In a recent paper, we dealt with the TL associated with a two-electron trap and a one-hole center. Here, we consider the case of one-electron traps and two-hole centers. A new set of simultaneous differential equations governing the three stages of excitation, relaxation and readout of TL in this new framework is developed. This situation is dealt with by solving these sets of equations sequentially for reasonable sets of chosen trapping parameters. Also, an analytical treatment using plausible simplifying assumptions is given in parallel. The outcome of these procedures yields a two-peak TL curve and, in a sense, to some extent, the two-hole center behaves as two centers with different recombination probabilities. The results of the simulations and the approximate analytical approach show that the lower-temperature peak has usually features of first-order peak and its intensity is superlinear with the dose of excitation. With the appropriate choice of parameters, the dose dependence of the first peak has been found to be initially quadratic with the excitation dose. This may explain experimental results of quadratic dose dependence previously reported in the literature. The second peak has second-order features and both peaks shift to lower temperatures with increasing dose. This effect is explained by a change in the effective frequency factor with the excitation dose.

### 1. Introduction

In a recent paper, Chen et al. (2017) have described a TL model consisting of a two-electron trap and a single-hole recombination center. The model explained the occurrence of two TL peaks, the first exhibiting first-order features and the second has second-order kinetics. The lower-temperature peak showed an initial steep superlinear dependence on the dose, cubic or somewhat steeper than cubic. The concepts of two-electron traps and two-hole centers have been mentioned in the literature for the explanation of different solid-state phenomena. Several solid-state phenomena have been explained to be associated with a two-electron trap model as described in the introduction of the paper by Chen et al. (2017). Of special interest is the paper by Woda and Wagner (2007) who, in an explanation of a non-monotonic dose dependence of Ge- and Ti-centers in quartz, discussed a model of double-electron capture which can be expressed in both ESR and TL measurements.

A somewhat similar situation of two-hole centers has been considered in the literature. Winter et al. (1969) reported on the dichroism

of V bands in potassium and rubidium halides and explained the results using a model of two holes trapped at an anion in a cation vacancy. More specifically, with regard to TL, Mayhugh (1970) and Townsend et al. (1979) explained results of thermoluminescence in LiF by the existence of  $V_3$  centers containing two trapped holes. Böhm and Scharmann (1981) mentioned the two-electron  $F'$  center in alkali-halides with relation to the general subject of TL dosimetry. Yazici et al. (2004) who studied TL of LiF:Mg, Ti between 100 and 300K suggested that their results are related to the  $V_3$  two-hole centers. The same  $V_3$  two-hole centers have been considered as being associated with TL by Horowitz (2006) and by Eliyahu et al. (2016).

In the present work we present a TL model of one electron trap and one hole recombination center, the latter capable of capturing two holes. It should be mentioned that it is convenient to speak about a two-electron trap as the entity which can release thermally or optically sequentially two electrons into the conduction band before their recombination with a stationary hole and about two-hole centers which can recombine sequentially with two free electrons from the conduction band. However, the mirror image situation of a single-hole trap and a

\* Corresponding author.

E-mail address: [chenr@tau.ac.il](mailto:chenr@tau.ac.il) (R. Chen).

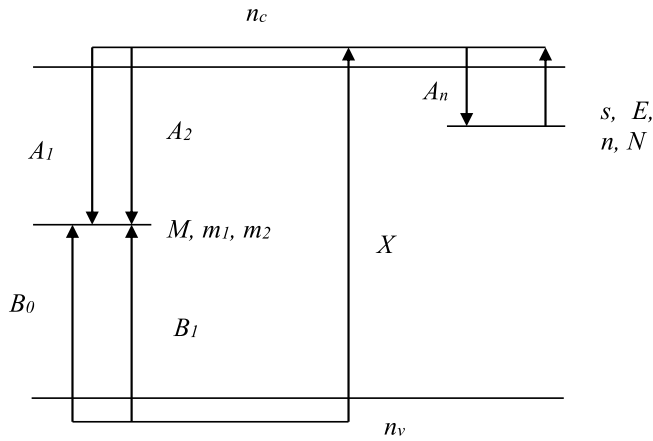


Fig. 1. Energy-level diagram of a model with an electron trap and a two-hole recombination center. The meaning of the different variables is given in the text.

double-electron center is feasible all the same. We will continue to talk about the two-hole luminescence centers, but will keep in mind that the inverse situation is possible. The sets of simultaneous differential equations governing the processes for these two sets of circumstances are exactly the same.

## 2. The model

The following model deals with one trap,  $N$  ( $\text{cm}^{-3}$ ), with an instantaneous occupancy of  $n$  ( $\text{cm}^{-3}$ ) and one center,  $M$  ( $\text{cm}^{-3}$ ), which may trap either one or two holes during excitation by irradiation. A schematic energy-level diagram of the model is shown in Fig. 1. The activation energy of electrons thermally raised into the conduction band is  $E$  (eV) and the frequency factor is  $s$  ( $\text{s}^{-1}$ ). The retrapping probability coefficient of an electron from the conduction band back to the trap is  $A_n$  ( $\text{cm}^3\text{s}^{-1}$ ).  $m_1$  ( $\text{cm}^{-3}$ ) is the instantaneous concentration of centers holding one hole and  $m_2$  ( $\text{cm}^{-3}$ ) is the concentration of centers with two holes.  $B_0$  ( $\text{cm}^3\text{s}^{-1}$ ) is the probability coefficient for trapping a hole in a neutral center and  $B_1$  ( $\text{cm}^3\text{s}^{-1}$ ) is the probability coefficient for trapping a hole in a center occupied by one hole.  $A_1$  ( $\text{cm}^3\text{s}^{-1}$ ) is the recombination probability coefficient of a free electron into a center occupied by a single hole and  $A_2$  ( $\text{cm}^3\text{s}^{-1}$ ) is the recombination probability coefficient into a center with two holes.  $X$  ( $\text{cm}^{-3}\text{s}^{-1}$ ) is the rate of production of electron-hole pairs by the irradiation, proportional to the dose rate. If the irradiation takes place for a time  $t_D$  (s), then  $D = X \cdot t_D$  ( $\text{cm}^{-3}$ ) is the total concentration of pairs produced, proportional to the total applied dose.  $n_c$  ( $\text{cm}^{-3}$ ) and  $n_v$  ( $\text{cm}^{-3}$ ) are respectively the instantaneous concentrations of free electrons and free holes.

The equations governing the process during excitation are:

$$\frac{dn}{dt} = A_n(N - n)n_c - sn \exp(-E/kT), \quad (1)$$

$$\frac{dm_1}{dt} = B_0n_v(M - m_1 - m_2) - B_1m_1n_v - A_1n_cm_1 + A_2n_cm_2, \quad (2)$$

$$\frac{dm_2}{dt} = B_1m_1n_v - A_2n_cm_2, \quad (3)$$

$$\frac{dn_v}{dt} = X - B_0(M - m_1 - m_2)n_v - B_1m_1n_v, \quad (4)$$

$$\frac{dn_c}{dt} = X - A_n(N - n)n_c - A_1m_1n_c - A_2m_2n_c + sn \exp(-E/kT). \quad (5)$$

Let us apply the initial conditions  $m_1(0) = m_2(0) = n(0) = 0$  and we get from these equations

$$n_c + n = n_v + m_1 + 2m_2. \quad (6)$$

Note that Eq. (6) is a charge balance condition. The factor of 2 in front of  $m_2$  indicates that, instantaneously,  $m_2$  centers hold two holes each. Equation (6) can be written in a differential way as

$$\frac{dn_c}{dt} = \frac{dm_1}{dt} + 2\frac{dm_2}{dt} + \frac{dn_v}{dt} - \frac{dn}{dt}. \quad (7)$$

If one wishes to simulate the TL process, it has to be done, as usual, in three stages. A set of parameters is to be chosen with a certain dose rate  $X$  and Eqs. (1)–(5) solved numerically for a certain period of time  $t_D$ . In the next stage of relaxation, one should set  $X = 0$ , use the last values of the first stage as initial values for the second stage and solve the same equations for a certain period of time so that  $n_c$  and  $n_v$  are reduced to practically zero. In the last stage of heating, a certain heating function  $T = T(t)$  is to be chosen, usually a linear function  $T = T_0 + \beta t$  where  $\beta$  ( $\text{Ks}^{-1}$ ) is the constant heating rate. The last values of the concentration functions in the second stage are to be used as initial values for the third stage. Also, during heating  $X$  is kept zero and therefore, in this stage,  $n_v = 0$  thus, Eq. (4) can be ignored.

## 3. Numerical simulations

It should be noted that the probability of capturing of the first hole in the center is expected to be larger than that of the second hole,  $B_0 > B_1$ , due to Coulombic repulsion. Also, one expects that  $A_2 > A_1$  since the Coulombic attraction of a free electron is stronger into a center with two holes than into one with a single hole. The emission of light can be associated with  $A_1m_1n_c$  or  $A_2m_2n_c$  or some weighted sum of the two. Let us denote the two emission peaks by  $I_1(t)$  and  $I_2(t)$  associated with the recombination of a free electron with a center with one hole and with two holes, respectively. These two intensities are given by

$$I_1(T) = A_1m_1n_c, \quad (8)$$

and

$$I_2(T) = A_2m_2n_c. \quad (9)$$

Note that these two transitions are expected to have different emission spectra and therefore, in the measurements, they can be separated using appropriate optical filters.

The parameters used for the simulation were:

$$B_0 = 10^{-9} \text{ cm}^3\text{s}^{-1}, \quad B_1 = 10^{-10} \text{ cm}^3\text{s}^{-1}, \quad A_n = 10^{-15} \text{ cm}^3\text{s}^{-1},$$

$$A_1 = 10^{-11} \text{ cm}^3\text{s}^{-1}, \quad A_2 = 10^{-10} \text{ cm}^3\text{s}^{-1}, \quad s = 10^{12} \text{ s}^{-1}, \quad E = 1.0 \text{ eV};$$

$$N = 10^{15} \text{ cm}^{-3}, \quad M = 10^{15} \text{ cm}^{-3}, \quad X = 10^{10} \text{ cm}^{-3}\text{s}^{-1}. \quad \text{The excitation time } t_D \text{ varied between } 0.125 \text{ and } 64 \text{ s. Practically the same results were reached by varying the dose rate. We kept the time at } 1\text{s}^{-1} \text{ and varied the dose rate between } 1.25 \times 10^8 \text{ and } 6.4 \times 10^{11} \text{ cm}^{-3}\text{s}^{-1}. \text{ A representative result is shown in Fig. 2. Curve (a) denotes a peak that occurs with the dose of } 1 \times 10^{10} \text{ cm}^{-3} \text{ at } 387 \text{ K. This peak results from the recombination of a free electron with a hole in a center holding two holes and associated with the transition-probability coefficient } A_2. \text{ The simulated intensity of this peak is significantly smaller than that of the other peak and in order to show both on the same scale it is multiplied by } 2 \times 10^6. \text{ Curve (b) shows the peak occurring at } 413 \text{ K with the same dose, resulting from a recombination of an electron with a single hole residing in the center and is associated with the transition probability } A_1. \text{ The order of appearance of the two peaks makes sense since the probability of recombination with a center with two holes is 10 times larger than that with a single hole in the center. As pointed out, these two transitions probably yield photons of different energies, so no exact comparison of the two intensities can be made.}$$

The lower temperature peak has symmetry of  $\mu_g \sim 0.424$ , characteristic of first-order kinetics. The activation energy of this peak has been found to be  $E_{\text{eff}} = 0.99$  eV, very close to the inserted value of 1.0 eV and the effective frequency factor  $s_{\text{eff}} = 8.4 \times 10^{10} \text{ s}^{-1}$ , about an order of magnitude smaller than the used value of  $s = 10^{12} \text{ s}^{-1}$ . The second peak has a symmetry factor of  $\mu_g \sim 0.55$ , typical of second-order

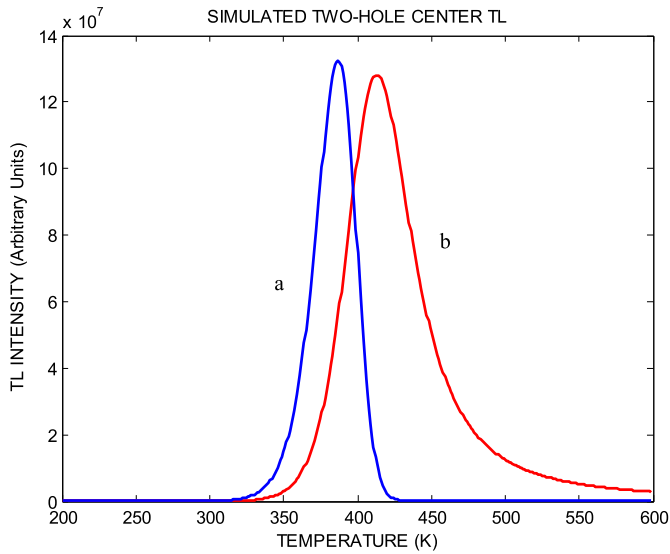


**Fig. 2.** A representative result of the numerically evaluated glow peaks. Curve (a) is a peak simulated with the dose of  $10^{10} \text{ cm}^{-3}$  at 387 K. This peak,  $I_2(T)$  results from the recombination of a free electron with a hole in a center holding two holes. Curve (b) is the peak at 413 K with the same dose, resulting from a recombination of an electron with a single hole residing in the center,  $I_1(T)$ . Note the very large difference in intensities; the results in curve (a) have been multiplied by  $2 \times 10^6$ . The parameters chosen for the simulation are given in the text.

peak. The activation energy of this peak found by the peak-shape method (Chen, 1969) has been  $E_{eff} = 0.94 \text{ eV}$ , also rather close to the inserted value and the effective frequency factor  $s_{eff} = 1.1 \times 10^{11} \text{ s}^{-1}$ , about an order of magnitude smaller than that used in the simulation. The values of the effective frequency factors will be discussed below. Also will be discussed the different possibilities of the symmetry factors and their meaning.

We have also simulated the dependence of these two peaks on the dose of excitation. The results of the dependence of  $I_m$ , the maximum intensity on the dose is shown in Fig. 3. Note that these results are practically the same for varying the dose by changing the dose rate  $X$  using the same time of excitation  $t_D$ , or by changing the time of excitation, keeping the dose rate constant. Curve (a) shows the dependence of the first peak intensity on the dose on a log-log scale. The simulated intensities have been multiplied by  $2 \times 10^6$ . The initial slope is about 2, i.e., quadratic dose dependence and it gets smaller, but still higher than unity at higher doses. It should be noted that this first-order looking peak behaves in an unusual way in the sense that within this range of doses, it shifts from 403 K at the lowest dose to 362 K, an unusual behavior for a first-order peak.

The dependence of the maximum intensity of the second peak on the dose is shown in curve (b) of Fig. 3. This dose dependence is rather characteristic of second-order peaks since  $I_m$  depends slightly super-linearly on the dose at the beginning and then continues approximately linearly before approaching saturation. The temperature of the peak shifts from 438 K to 387 K in this range of doses. This kind of shift is typical of second-order peaks though the amount of shift looks somewhat larger than expected.

In order to try to understand the dose dependence of these peaks, we have recorded the concentrations of electrons and holes in traps and centers at the end of the relaxation stage, prior to heating. The results are shown in Fig. 4 on log-log scale. The concentrations of trapped electrons and holes,  $n_0 = m_{10}$  is shown in red and that of centers with one hole,  $m_{20}$ , in blue. The line of  $n_0$  and  $m_{10}$  starts linearly at low doses and gets slightly sublinear at higher doses. The line of  $m_{20}$  starts with a slope of  $\sim 2$ , describing quadratic dose dependence, and its slope reduces at higher doses, but is more than unity all along, indicating

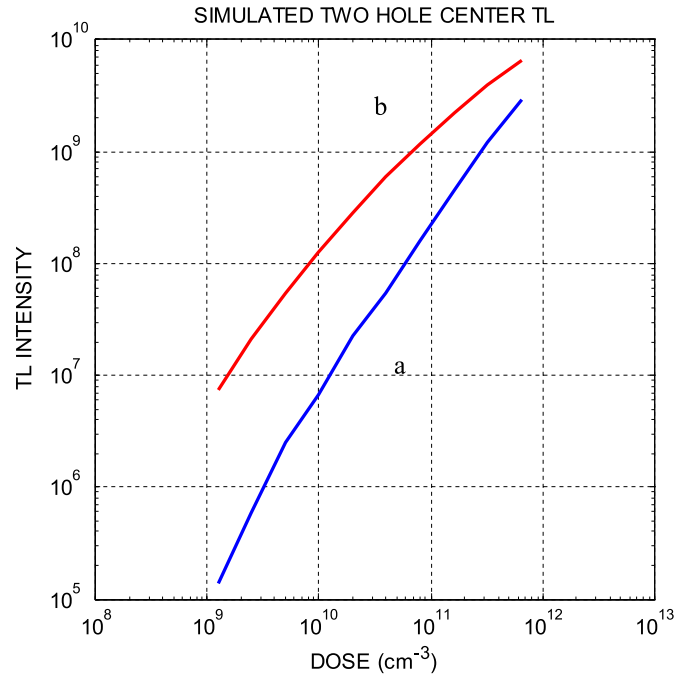


**Fig. 3.** The dependence of the maximum intensity of the two simulated peaks on the dose, given on a log-log scale. Curve (a) shows the results for the first peak (transitions into  $m_2$ ) and curve (b), the second peak. The parameters used for simulation are the same as in Fig. 2. The results in curve (a) have been multiplied by  $10^5$ .

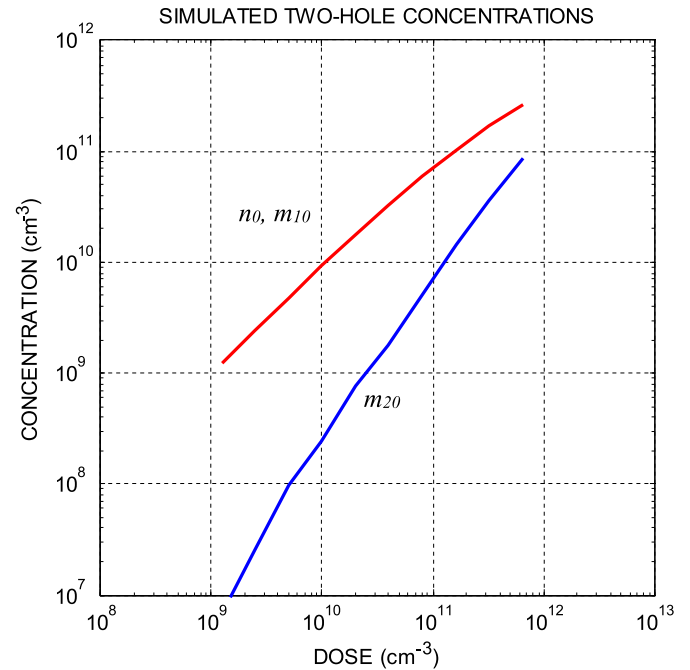


**Fig. 4.** Dose dependence of the concentrations  $n_0$ ,  $m_{1,0}$  and  $m_{2,0}$ , the occupancies of the traps and the single-hole and double-hole centers. The parameters used for simulation are the same as in Fig. 2. The results of  $m_{20}$  were multiplied by  $2 \times 10^6$ .

superlinear dose dependence. The similarity between the shapes of Figs. 3 and 4 indicates that the dose dependence of the simulated first TL peak is directly related to the concentration of holes in  $m_2$  and that of the second peak relates to the concentration of  $m_1$  both at the beginning of the heating stage.

In order to get some insight into the behavior of the one-hole and

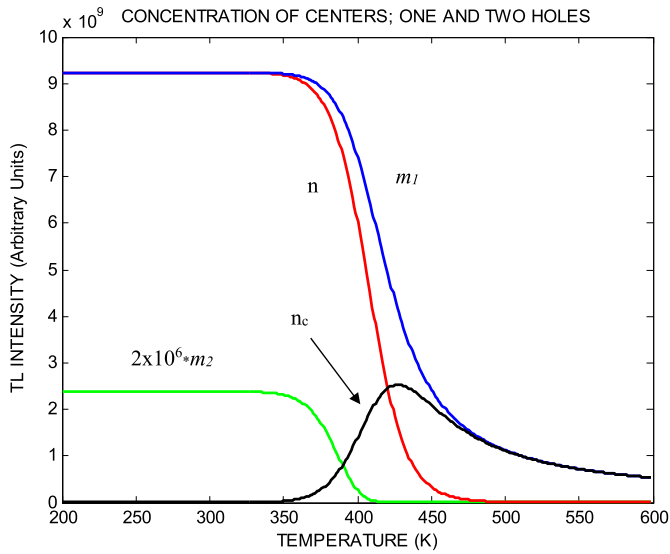


Fig. 5. Variation of the relevant occupancies,  $n$ ,  $m_1$ ,  $m_2$  and  $n_c$  with temperature as simulated with the same set of parameters as before. The concentrations  $n$ ,  $m_1$ ,  $m_2$  decrease in the range of occurrence of the TL peaks.  $n_c$  is a peak-shaped function with a maximum at 428K.

two-hole occupancies during the process, we have printed out the simulated concentrations as a function of temperature. Fig. 5 shows the dependence of the concentration of electrons in traps and holes in centers as well as that of free electrons as a function of temperature. The concentration of holes in two-hole centers associated with the first peak decreases from its initial value to practically zero between  $\sim 350$  K and  $\sim 410$  K. With the given parameters, the concentration of  $m_2$  is significantly lower than that of  $m_1$  which results in a big difference between the intensities of the two peaks. As for the concentration of free electrons,  $n_c$ , it starts rising at  $\sim 350$  K, in the range where the trapped electrons concentration  $n$  starts to decrease.  $n_c$  then reaches a maximum at  $\sim 428$  K and then decreases rather slowly. It is interesting to note that the TL peaks seen at Fig. 2 occur at lower temperature than the peak of  $n_c$ , which agrees with the theory previously reported (Chen, 1971) predicting that usually, TL peaks precede their thermally stimulated conductivity (TSC) counterparts.

## 4. Theoretical account

### 4.1. The excitation stage

We can assume that the excitation takes place at a low enough temperature, well before the occurrence of the emitted TL and therefore, the exponential term in Eqs. (1) and (5) can be assumed to be nil. Let us assume that the lifetime of free electrons and free holes is much shorter than the irradiation lifetime. Since irradiation typically takes place over seconds or even years and the lifetimes are often measured in microseconds, this is generally a good approximation. As a consequence, the free electron and free hole populations can be given by

$$n_c = \frac{X}{A_n(N-n) + A_1m_1 + A_2m_2}, \quad (10)$$

$$n_v = \frac{X}{B_0(M-m_1-m_2) + B_1m_1}. \quad (11)$$

In Eqs. (10) and (11), the numerator represents the production rate of free electrons and holes and the denominators represent terms for their capture. The governing equations then reduce to

$$\frac{dn}{dt} = \frac{A_n(N-n)}{A_n(N-n) + A_1m_1 + A_2m_2}X, \quad (12)$$

$$\frac{dm_1}{dt} = \frac{B_0(M-m_1-m_2) - B_1m_1}{B_0(M-m_1-m_2) + B_1m_1}X + \frac{A_2m_2 - A_1m_1}{A_n(N-n) + A_1m_1 + A_2m_2}X, \quad (13)$$

$$\frac{dm_2}{dt} = \frac{B_1m_1}{B_0(M-m_1-m_2) + B_1m_1}X - \frac{A_2m_2}{A_n(N-n) + A_1m_1 + A_2m_2}X. \quad (14)$$

Let us discuss Eq. (12). After irradiation creates a free electron, three things can happen to it. It can (i) be captured by a trap, (ii) recombine into a center with one hole, or (iii) recombine into a center with two holes. The relative rates for these three processes are  $A_n(N-n)$ ,  $A_1m_1$  and  $A_2m_2$ . Thus, the fraction of electrons that are captured by the trap is  $A_n(N-n)$  divided by the sum of  $A_n(N-n)$ ,  $A_1m_1$  and  $A_2m_2$ . The rate of increase of the trapped population  $dn/dt$  is the rate at which the free electrons are created,  $X$ , times the fraction of those electrons,  $A_n(N-n)/[A_n(N-n) + A_1m_1 + A_2m_2]$ , which do not recombine at a center but instead are captured by the trap.

Equation (14) is similar except that both free holes and free electrons affect the population of  $m_2$ . The first term on the right-hand side of Eq. (14) is the rate of free hole production,  $X$ , multiplied by the fraction of free holes that are captured by the center with one hole. The second term on the right-hand side represents the rate of loss of  $m_2$  due to recombination. It is the rate of free electron production,  $X$ , times the fraction of those free electrons which recombine with  $m_2$ .

Equation (13) is similar except that there are four relevant processes. The first two are (i) hole capture by the empty center creating  $m_1$  and (ii) hole capture by  $m_1$  depleting  $m_1$ . These two processes are represented in the first term on the right-hand side of Eq. (13). The other two processes are (iii) electron recombination with  $m_2$  which increases  $m_1$  and (iv) electron recombination with  $m_1$  which depletes the  $m_1$  population. These two processes are represented by the second term on the right-hand side of Eq. (13). Eqs. (12)–(14) can be combined to again yield the conservation of charge

$$m_1 + 2m_2 = n, \quad (15)$$

which is the same as Eq. (6) where  $n_c$  and  $n_v$  are negligibly small as compared to the other occupancies.

### 4.2. The low dose range

To obtain the populations of  $n$ ,  $m_1$  and  $m_2$  in the low dose range, let us expand their concentrations in Taylor series at  $t = 0$ . Starting with  $n$ ,

$$n = n \Big|_{t=0} + \frac{dn}{dt} \Big|_{t=0} t + \dots = 0 + Xt + \dots, \quad (16)$$

where we used Eq. (12) to evaluate  $dn/dt|_{t=0}$ . Since  $D = Xt$ , Eq. (16) reduces to

$$n = D + O(D^2). \quad (17)$$

This indicates that initially, all free electrons created by the irradiation are captured by the electron trap,  $n$ . This is a consequence of the initial hole concentrations  $m_1$  and  $m_2$ , being zero and thus providing no competition to capture by the trap.

Similarly, we can determine the initial growth of  $m_1$

$$m_1 = m_1|_{t=0}t + \dots = 0 + Xt + \dots, \quad (18)$$

where Eq. (13) was used to evaluate the derivative. As before, using  $D = Xt$ , this yields

$$m_1 = D + O(D^2). \quad (19)$$

This indicates that initially, all free holes created by irradiation are captured by empty centers to form  $m_1$  type one-hole centers.

Solving for  $m_2$  is similar except that we need to take the first three terms of the Taylor series

$$m_2 = m_2 \Big|_{t=0} + \frac{dm_2}{dt} \Big|_{t=0} t + \frac{d^2m_2}{dt^2} \Big|_{t=0} \frac{t^2}{2} + \dots = 0 + 0 + \frac{B_1 X}{B_0 M} \frac{dm_1}{dt} \Big|_{t=0} \frac{t^2}{2} + \dots, \quad (20)$$

and therefore,

$$m_2 = \frac{B_1 X^2 t^2}{B_0 M 2}, \quad (21)$$

where Eq. (20) was obtained by differentiating Eq. (14) and Eq. (21) by substituting Eq. (13) and evaluating at  $t = 0$ .

Again, using  $D = Xt$ , we have

$$m_2 = \frac{B_1 D^2}{B_0 2M} + O(D^3). \quad (22)$$

This shows for low doses a quadratic dependence of  $m_2$  on the dose  $D$ . The reason seems to be that it is not possible to capture holes in  $m_2$  until a nonzero population of  $m_1$  has been created.

### 4.3. The heating stage

Let us consider the relevant equations and their solution during the heating stage. Here,  $n_v = 0$  and, consequently, the governing equations simplify to

$$\frac{dn}{dt} = A_n(N - n)n_c - ns \exp(-E/kT), \quad (23)$$

$$\frac{dm_1}{dt} = -A_1 m_1 n_c + A_2 m_2 n_c, \quad (24)$$

$$\frac{dm_2}{dt} = -A_2 m_2 n_c, \quad (25)$$

$$\frac{dn_c}{dt} = ns \exp(-E/kT) - A_n(N - n)n_c - A_1 m_1 n_c - A_2 m_2 n_c. \quad (26)$$

Assuming, as usual, that the free electron lifetime is much shorter than the characteristic heating time, the free electron density from Eq. (26) reduces to

$$n_c = \frac{ns \exp(-E/kT)}{A_n(N - n) + A_1 m_1 + A_2 m_2}. \quad (27)$$

As a consequence, Eqs. (23)–(25) reduce to

$$\frac{dn}{dt} = -\frac{A_1 m_1 + A_2 m_2}{A_n(N - n) + A_1 m_1 + A_2 m_2} ns \exp(-E/kT), \quad (28)$$

$$\frac{dm_1}{dt} = \frac{A_2 m_2 - A_1 m_1}{A_n(N - n) + A_1 m_1 + A_2 m_2} ns \exp(-E/kT), \quad (29)$$

$$\frac{dm_2}{dt} = -\frac{A_2 m_2}{A_n(N - n) + A_1 m_1 + A_2 m_2} ns \exp(-E/kT). \quad (30)$$

With these equations, we could determine the intensity profiles for radiative recombination into either  $m_1$  or  $m_2$ . For our purposes,  $m_2$  is more interesting and we will examine it.

For low doses, we know from the theory for irradiation that

$$m_2 < m_1. \quad (31)$$

Based on charge differences, as pointed out above, one expects that the following is generally true

$$A_1 < A_2. \quad (32)$$

As will be shown in the appendix, a consequence of conditions (31) and (32) is that  $m_2$  will deplete much faster than  $m_1$ , which can be seen in Fig. 5. Thus, while  $m_2$  is depleting,  $m_1$  and  $n$  remain at approximately their initial values  $m_{1,0}$  and  $n_0$ , respectively. Note that because of the inequality (31), we have  $m_{1,0} \approx n_0$ .

Let us consider now two possibilities. The first, Case 1, is to assume that the dose is low enough so that

$$A_2 m_2 \ll A_n(N - n) + A_1 m_1. \quad (33)$$

Alternatively, as Case 2, we could assume, for example, that

$$2A_n = A_2. \quad (34)$$

In either case 1 or case 2, Eq. (30) can be written as

$$\frac{dm_2}{dt} = -s_{eff} m_2 \exp(-E/kT), \quad (35)$$

where

$$s_{eff} = \frac{A_2 m_{1,0} s}{A_n(N - m_{1,0}) + A_1 m_{1,0}}. \quad (36)$$

With  $s_{eff}$  approximately constant, Eq. (35) is a first-order equation characterized by activation energy  $E$  and pre-exponential  $s_{eff}$ . As observed from Eq. (36),  $s_{eff}$  is dose dependent. The existence of these two cases leading to the same conclusion is reminiscent of the Garlick-Gibson theory for second-order peaks. In the latter, the second-order kinetics was reached by either assuming a strong retrapping as compared to recombination or by assuming that the retrapping probability coefficient and the recombination probability coefficient are equal.

## 5. Discussion

In the present work, the situation of having a recombination center with one or two trapped holes is considered with regard to thermoluminescence. This possibility has been mentioned in the literature for different solid state phenomena and also specifically, for TL ( $V_3$  centers in LiF). The model discussed here bears some resemblance to the previously presented model of two-electron traps and their effect on TL, but some important differences take place. For a given set of parameters the model yields two peaks that are expected to have different emission spectra. Simulations show that the first peak has first-order features and the second peak is of second order. This is similar to previously discussed cases of a series of TL peaks resulting from a series of traps and a single recombination center (see e.g. Chen and Pagonis, 2013). It also resembles the behavior of the two peaks resulting from a system with a two-electron trap and one-hole center. However, here both the first-order and the second-order peaks shift with the dose of excitation to lower temperatures which is explained in the present case by showing that the effective frequency factor increases with the dose of excitation. Note, however, that according to Eq. (36), the rate of change of  $s_{eff}$  with the dose depends on the relative magnitude of  $A_2$  and  $A_1$ . For the simulations, we have chosen  $A_2$  ten times larger than  $A_1$ . It is possible that in real life situations, the difference between these probabilities is smaller, which would result in a smaller change of  $s_{eff}$  with the dose and therefore, a smaller variation of the temperature of the TL maximum with the dose. Note that some experimental works reported on a shift of TL peaks with first-order shape to lower temperature with increasing dose. Miallier et al. (1991) reported the effect in quartz, Gastéllum et al. (2007) reported it in diamond films and Nandha Gopal et al. (2016) in  $\text{CaSO}_4 \cdot \text{Dy}$ .

It is worth mentioning that the classification here of the mentioned peaks as first-order and second-order relies on the shape of the peaks, namely, that a first order peak is asymmetric with a symmetry factor  $\mu_g \sim 0.42$  and a second-order peak is nearly symmetric with  $\mu_g \sim 0.52$ . This does not mean that in the former case, the simple Randall-Wilkins first-order equation necessarily governs the process or that in the latter case, the Garlick-Gibson second-order equation exactly holds. The process is obviously governed by the whole set of equations, and while trying different sets of parameters and different simulated doses, intermediate cases of the symmetry have been observed. In this sense, intermediate order of kinetics was encountered, which could be translated into an effective intermediate order of kinetics between 1 and 2.

The shift of the peaks with the simulated magnitude of the dose should be considered. In the simulations, the shift has been up to 50 K.



In many cases of experimental results, this shift is smaller, however. Orante-Barrón et al. (2015) have reported such a shift of a TL peak in ZnO nanophosphors. Also, Sharma and Gosavi (2014) have communicated on a large shift of the TL peak with the dose of excitation in graphene-nano ZnS composite samples.

Similarly to cases of competition between two traps or centers (see e.g. Kristianpoller et al., 1974; Bowman and Chen, 1979; Chen and Fogel, 1993; Chen et al., 1996), the dose dependence of the first peak here is superlinear. This superlinearity is quadratic at low doses and less than quadratic at higher doses, less drastic than the results of the two-electron trap model (Chen et al., 2017) and some experimental results mentioned therein (Halperin and Chen, 1966; Otaki et al., 1994; Chen et al., 1988). The second peak is only slightly superlinear with the dose, similarly to “regular” second-order peaks (Chen et al., 1983). It is worth mentioning that the initial quadratic dose dependence of both the concentration  $m_2$  and the intensity of the first peak indicate that this dose dependence of TL is associated with the process taking place

## Appendix

Let us compare the time it takes during heating for  $m_1$  and  $m_2$  to deplete. To begin with, let us create a stretched-time  $\tau$  defined by

$$\tau = \int_0^t \frac{n(t')}{n_0} \frac{s \exp[-E/kT(t')]}{A_n [N - n(t')] + A_1 m_1(t') + A_2 m_2(t')} dt', \quad (\text{A1})$$

where  $t'$  is the variable of integration and in the integrand,  $T$ ,  $n$ ,  $m_1$  and  $m_2$  are all to be evaluated at time  $t'$ .  $n_0$  is the population of  $n$  at the start of heating,  $t = 0$ . With this definition for  $\tau$ , Eqs. (29) and (30) can be written as

$$\frac{dm_1}{d\tau} = A_2 n_0 m_2 - A_1 n_0 m_1, \quad (\text{A2})$$

$$\frac{dm_2}{d\tau} = -A_2 n_0 m_2. \quad (\text{A3})$$

This system of two coupled differential equations in two variables has the solution

$$m_1 = \left( m_{1,0} + \frac{m_{2,0}}{1 - A_1/A_2} \right) \exp(-A_1 n_0 \tau) - \frac{m_{2,0}}{1 - A_1/A_2} \exp(-A_2 n_0 \tau), \quad (\text{A4})$$

$$m_2 = m_{2,0} \exp(-A_2 n_0 \tau). \quad (\text{A5})$$

As pointed out above, based on the relative charges one expects that  $A_1 < A_2$ . Consequently, the expression  $\exp(-A_2 n_0 \tau)$  will drop to zero much faster than  $\exp(-A_1 n_0 \tau)$ . From Eq. (A5), we thus see that  $m_2$  will rapidly drop to zero. During the time that  $m_2$  drops to zero,  $m_1$  experiences an increase in population of approximately  $m_{2,0}$ . For low doses,  $m_2 < m_1$  and therefore, this increase is negligible. After that and governed by the size of  $A_1$ ,  $m_1$  experiences a slow decline to zero. The simulated results with the same set of parameters of  $m_1$  and  $m_2$  are shown in Fig. 5.

## References

- Böhm, M., Scharmann, A., 1981. In: Oberhofer, M., Scharmann, A. (Eds.), Theory, Applied Thermoluminescence Dosimetry, vol. 2. pp. 11–38 Ch.
- Bowman, S.G.E., Chen, R., 1979. Superlinear filling of traps in crystals due to competition during heating. *J. Lumin.* 18/19, 345–348.
- Chen, R., 1969. On the calculation of activation energies and frequency factors from glow curves. *J. Appl. Phys.* 40, 570–585.
- Chen, R., 1971. Simultaneous measurement of thermally stimulated conductivity and thermoluminescence. *J. Appl. Phys.* 42, 5899–5901.
- Chen, R., Huntley, J.R., Berger, G.W., 1983. Analysis of TL data dominated by second-order kinetics. *Phys. Status Solidi* 79, 251–261.
- Chen, R., Yang, X.H., McKeever, S.W.S., 1988. The strongly superlinear dose dependence of thermoluminescence in synthetic quartz. *J. Phys. D Appl. Phys.* 21, 1452–1457.
- Chen, R., Fogel, G., 1993. Superlinearity in thermoluminescence revisited. *Radiat. Protect. Dosim.* 47, 23–26.
- Chen, R., Fogel, G., Lee, C.K., 1996. A new look at the models of the superlinear dose dependence of thermoluminescence. *Radiat. Protect. Dosim.* 65, 63–68.
- Chen, R., Pagonis, V., 2013. On the expected order of kinetics in a series of thermoluminescence (TL) and thermally stimulated conductivity (TSC) peaks. *Nucl. Instrum. Meth. Phys. Res.* B312, 60–69.
- Chen, R., Lawless, J.L., Pagonis, V., 2017. Thermoluminescence associated with two-electron traps. *Radiat. Meas.* 99, 10–17.
- Eliyahu, I., Druzhyina, S., Horowitz, Y., Reshes, G., Biderman, S., Oster, L., 2016. Kinetic simulation of charge transfer following 5.08 eV (F band) optical excitation of irradiated LiF:Mg,Ti (TLD-100): participation of holes released via  $V_3$ - $V_k$  transformation. *Radiat. Meas.* 90, 27–32.
- Gastélum, S., Cruz-Zaragoza, E., Meléndez, R., Chernov, V., Barboza-Flores, M., 2007. Dose rate effects on the thermoluminescence properties of MWCD diamond films. *Radiat. Eff. Defect Solid* 162, 587–595.
- Halperin, A., Chen, R., 1966. Thermoluminescence of semiconducting diamonds. *Phys. Rev.* 148, 839–845.
- Horowitz, Y., 2006. A unified and comprehensive theory of the TL dose response of thermoluminescent systems applied to LiF:Mg,Ti. In: Horowitz, Y. (Ed.), Microdosimetric Response of Physical and Biological Systems to Low- and High-LET Radiations. Elsevier, Amsterdam, pp. 75–202.
- Kristianpoller, N., Chen, R., Israeli, M., 1974. Dose dependence of thermoluminescence peaks. *J. Phys. D Appl. Phys.* 7, 1063–1072.
- Mayhugh, M.R., 1970. Color centers and the thermoluminescence mechanism in LiF. *J. Appl. Phys.* 41, 4776–4782.
- Miallier, D., Faïn, J., Montret, T.H., Sanzelle, S., Soumana, S., 1991. Properties of the red TL peak of quartz relevant to thermoluminescence dating. *Nucl. Tracks Radiat. Meas.* 18, 89–94.
- Nandha Gopal, J., Sanyal, Bhaskar, Lakshmanan, Arunachalam, 2016. Thermoluminescence of high sensitive microcrystalline  $\text{CaSO}_4$ :Dy for high dose measurements. *Int. J. Lumin. Appl.* 6, 14–19.
- Orante-Barrón, V.R., Escobar-Ochoa, F.M., Cruz-Vázquez, C., Bernal, R., 2015. Thermoluminescence of novel zinc oxide nanophosphors obtained by glycine-based solution combustion synthesis. *J. Nanomater.* 2015 273571, 5pp.
- Otaki, H., Kido, H., Hiratsuka, A., Fukuda, Y., Takeuchi, N., 1994. Estimation of UV radiation dose using  $\text{CaF}_2$ :Tb, $\text{Dy}$  as a thermoluminescence dosimeter. *J. Mater. Sci. Lett.* 13, 1267–1269.
- Sharma, G., Gosavi, S.W., 2014. Thermoluminescence properties of graphene-nano ZnS composite. *J. Lumin.* 145, 557–562.
- Townsend, P.D., Taylor, G.C., Wintersgill, M.C., 1979. An explanation of the anomalously high activation energies of TL in LiF (TLD 100). *Radiat. Eff.* 41, 11–16.
- Winter, E.M., Wolfe, D.R., Christy, R.W., 1969. Dichroism of V bands in potassium and rubidium halides. *Phys. Rev.* 186, 949–952.
- Woda, C., Wagner, G.A., 2007. Non-monotonic dose dependence of the Ge- and Ti-centers in quartz. *Radiat. Meas.* 42, 1441–1452.
- Yazici, A.N., Karali, T., Townsend, P.D., Ari, M., 2004. Thermoluminescence studies of LiF:Mg,Ti between 100 and 300K. *J. Phys. D Appl. Phys.* 37, 3165–3173.